ORGANOMETALLICS

ARTICLE

pubs.acs.org/Organometallics

α-Cleavage of Phenyl Groups from $GePh_3$ Ligands in Iridium Carbonyl Cluster Complexes. A Mechanism and Its Role in the Synthesis of Bridging Germylene Ligands

Richard D. Adams,* Fang Fang, and Qiang Zhang

Department of Chemistry and Biochemistry, University of South Carolina, Columbia, South Carolina 29208, United States

Michael B. Hall* and Eszter Trufan

Department of Chemistry, Texas A&M University, College Station, Texas 77843, United States

Supporting Information

ABSTRACT: At 110 °C, the compound $HIr(CO)_3(GePh_3)_2$ (**1**) was decarbonylated and transformed into five polynuclear iridium compounds, $Ir_2(CO)_6(\mu\text{-}GePh_2)(GePh_3)_2$ (**2**), $Ir_3(CO)_6(\eta^1\text{-}Ph)_2(\mu\text{-}GePh_2)_3(GePh_3)$ (**3**), $Ir_3(CO)_6(\eta^1\text{-}Ph)(\mu\text{-}GePh_2)_3(GePh_3)_2$ (**4**), $Ir_3(CO)_6(\mu\text{-}CO)(\mu\text{-}GePh_2)_2(GePh_3)_3$ (**5**), and $Ir_3(CO)_6(\eta^1\text{-}Ph)(\mu\text{-}GePh_2)_2(GePh_3)_2[\mu\text{-}Ge(Ph)(OH)]$ (**6**), by a combination of condensation and phenyl-cleavage processes. The triiridium compounds **3**−**6** are all new and have been characterized by single-crystal X-ray diffraction analyses. Each new compound consists of a closed triangular cluster of three iridium atoms with two or three diphenylgermylene ligands bridging the Ir−Ir bonds. Separately, compound **5** was converted to **4** in 68% yield by decarbonylation and cleavage of a phenyl group from one of its $GePh_3$ ligands by heating a toluene solution to reflux (110 °C) for 1 h. A computational study has revealed that the mechanism of transformation of **5** to **4** occurs by elimination of the bridging carbonyl ligand followed by a "deinsertion" α-cleavage of a phenyl group from one of the $GePh_3$ ligands.

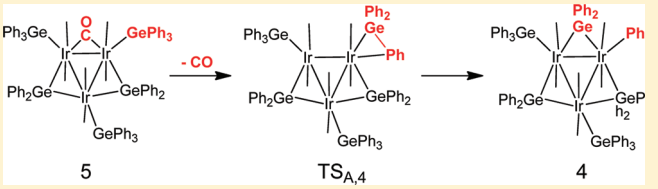

INTRODUCTION

The cleavage of phenyl groups from tertiary phosphines in their reactions with polynuclear metal complexes has resulted in the synthesis of a wide range of metal cluster complexes containing bridging phosphido (PPh_2) and phosphinidene (PPh) ligands.[1] The degradation of phosphine ligands is believed to play an important role in the deactivation of catalysts that contain these ligands.[2] Phenyl groups are also readily cleaved from $SbPh_3$ and $BiPh_3$.[3,4] Cleavage of phenyl groups from $SnPh_3$ and $GePh_3$ ligands leads to the formation of bridging stannylene ($SnPh_2$) and bridging germylene ($GePh_2$) ligands in polynuclear metal complexes.[5,6] If the complexes contain hydride ligands, the phenyl groups are generally expelled from the product in the form of benzene (see eq 1, where the CO ligands are shown by lines only).[5a] Sometimes, a phenyl group will remain as a ligand in the complex, as was observed in the products obtained when the compound $IrRu_3(CO)_{11}(GePh_3)_3(\mu\text{-}H)_4$ was heated to 68 °C (eq 2).[6]

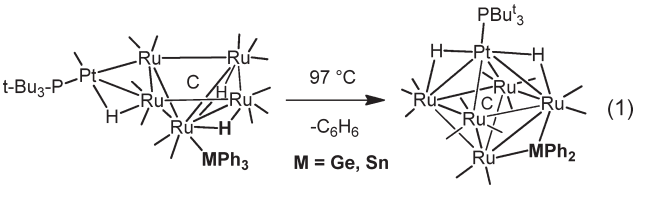

(1)

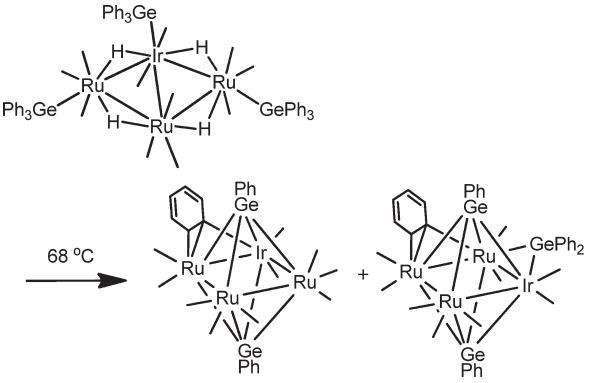

(2)

Tilley et al. has shown that α-cleavage of phenyl groups from $SnPh_3$ ligands in hafnium complexes can lead to metal complexes containing σ-phenyl groups by elimination of the $SnPh_2$ group (e.g. eq 3).[7] They described the transformation as α-elimination, and their kinetics studies were consistent with a process that occurs by an intramolecular phenyl migration mechanism.[7]

Special Issue: F. Gordon A. Stone Commemorative Issue

Received: July 28, 2011
Published: September 15, 2011

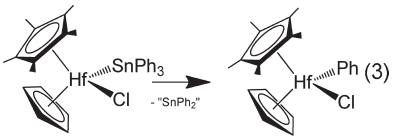

We have recently been investigating the synthesis and structures of polynuclear metal carbonyl complexes containing bridging phenyltin and phenylgermanium ligands by using $HSnPh_3$ and $HGePh_3$ reagents.[8,9] Polynuclear metal complexes containing bridging stannylene ($SnPh_2$) and bridging germylene ($GePh_2$) ligands have been prepared (e.g. eqs 4[8] and 5[9]). Some of these tin-containing complexes were found to serve as precursors to interesting bimetallic heterogeneous catalysts when they were placed on supports and were activated by the removal of their ligands.[10]

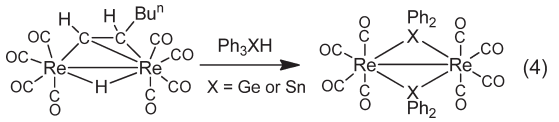

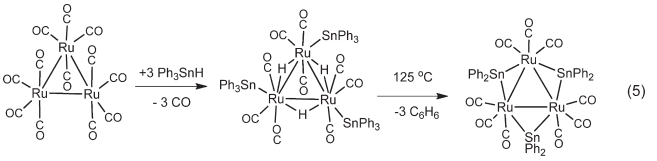

The catalytic properties of iridium have been of interest ever since Sinfelt showed that platinum−iridium nanoclusters exhibited superior catalytic properties in petroleum reforming processes.[11] Recently, iridium cluster catalysts have been shown to exhibit high activity for catalytic hydrogenation and dehydrogenation reactions.[12] Homogeneous catalysis by iridium complexes continues to grow in importance.[13] Today iridium is that catalyst of choice for the synthesis of acetic acid by the carbonylation of methanol.[14] The addition of germanium to iridium catalysts has been shown to improve the selectivity for aromatization, isomerization, and hydrocracking reactions in petroleum reforming processes.[15] Iridium−germanium catalysts have also been shown to exhibit improved selectivity for the hydrogenation of citral and other related unsaturated hydrocarbons.[16]

To date there have been very few reports of iridium carbonyl complexes containing organogermanium ligands.[17−19] Accordingly, we have recently been investigating the syntheses of polynuclear iridium complexes containing germanium ligands for their potential use as precursors to new heterogeneous nanocatalysts.[18,19] The reaction of $Ir_4(CO)_{12}$ with $HGePh_3$ has yielded a number of polynuclear iridium−germanium carbonyl cluster complexes containing bridging $GePh_2$ and GePh ligands (see Scheme 1; CO ligands are shown as lines only).[18]

The reaction of $[Ir(COD)(\mu\text{-Cl})]_2$ with triphenylgermane in the presence of CO has recently been found to yield the mononuclear bis(triphenylgermyl)iridium carbonyl complex $HIr(CO)_3(GePh_3)_2$ (**1**).[19] When heated, compound **1** is transformed into a number of diiridium carbonyl complexes containing terminal triphenylgermyl and bridging diphenylgermylene ligands (see Scheme 2).

We have now obtained several new triiridium carbonyl cluster compounds, $Ir_3(CO)_6(\eta^1\text{-Ph})_2(\mu\text{-GePh}_2)_3(GePh_3)$

Scheme 2. Synthesis and Reactions of $HIr(CO)_3(GePh_3)_2$ (1)[19]

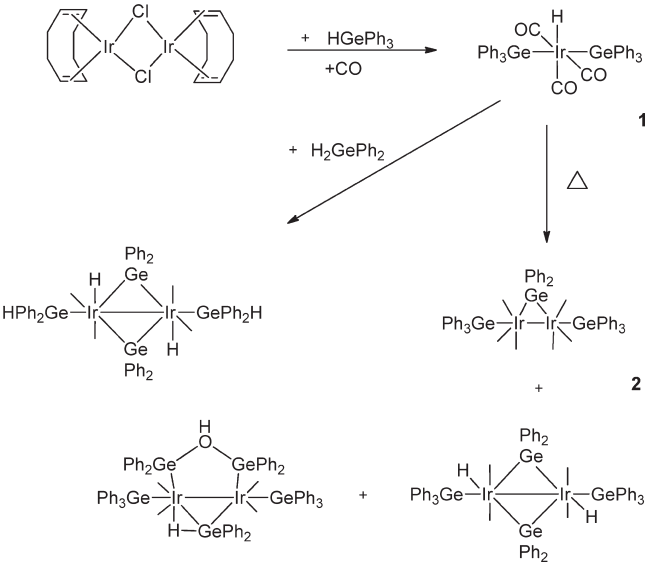

Scheme 1. Reaction of $Ir_4(CO)_{12}$ with $HGePh_3$ at Different Temperatures[18]

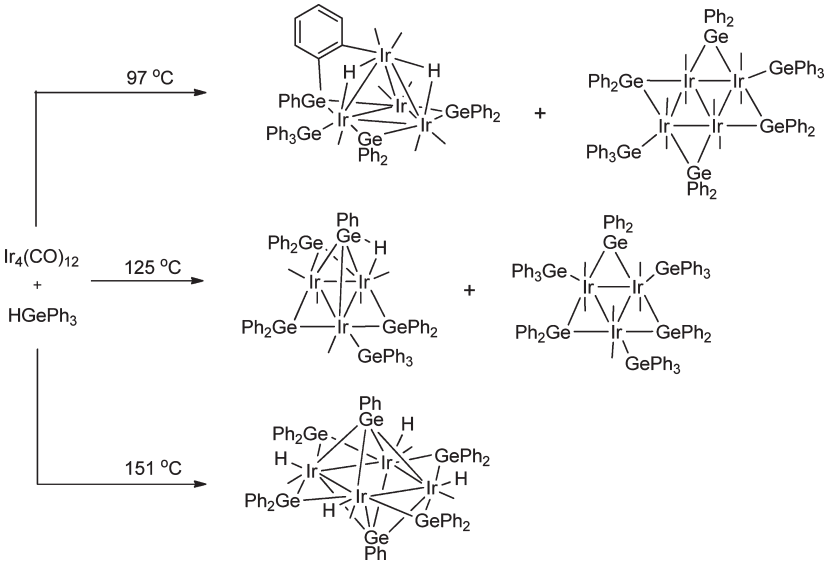

(**3**), $Ir_3(CO)_6(\eta^1\text{-Ph})(\mu\text{-GePh}_2)_3(GePh_3)_2$ (**4**), $Ir_3(CO)_6(\mu\text{-CO})(\mu\text{-GePh}_2)_2(GePh_3)_3$ (**5**), and $Ir_3(CO)_6(\eta^1\text{-Ph})(\mu\text{-GePh}_2)_2(GePh_3)_2[\mu\text{-Ge(Ph)(OH)}]$ (**6**), by controlled thermal transformations of **1** at 110 °C. All of the products contain bridging $GePh_2$ ligands formed by cleavage of phenyl rings from the $GePh_3$ ligands of **1**. Most importantly, we have found that compound **5** can be decarbonylated to **4** in good yield by the α-cleavage of a phenyl group from one of its $GePh_3$ ligands. The $GePh_2$ group that was formed was converted into a bridging $GePh_2$ ligand. A computational analysis has revealed that the mechanism of transformation of **5** to **4** occurs by an initial loss of the bridging carbonyl ligand followed by a migratory "deinsertion" α-cleavage of a phenyl group from a $GePh_3$ ligand.

EXPERIMENTAL SECTION

General Data. All reactions were performed under a nitrogen atmosphere unless otherwise specified. Reagent grade solvents were dried by standard procedures and were freshly distilled prior to use. Infrared spectra were recorded on a Thermo-Nicolet Avatar 360 FT-IR spectrophotometer. ^{1}H NMR spectra were recorded on a Mercury 300 spectrometer operating at 300.1 MHz. Mass spectrometric (MS) measurements performed either by direct-exposure probe using electron impact ionization (EI) or electrospray techniques (ES) were made on a VG 70S instrument. Product separations were performed by TLC in air on Analtech 0.25, 0.5, and 1.0 mm silica gel 60 Å F_{254} glass plates. $[Ir(COD)Cl]_2$ was purchased from Strem Chemicals Inc. and was used without further purification. $HGePh_3$ was purchased from Sigma-Aldrich and was used without further purification. $HIr(CO)_3(GePh_3)_2$ (**1**) was prepared by a modification of the previously reported procedure[19] (see the Supporting Information). $Ir_2(CO)_6(\mu\text{-GePh}_2)(GePh_3)_2$ (**2**) was also prepared as previously reported.[19]

Thermolysis of $HIr(CO)_3(GePh_3)_2$ (1) at 110 °C. A 26.3 mg portion (0.030 mmol) of **1** was dissolved in 20 mL of toluene to form a colorless solution in a 100 mL three-neck flask. The solution was refluxed for 2.5 h at 110 °C. During this time, the solution turned orange-red. The solvent was then removed in vacuo, and the products were separated by TLC by using a 2:1 hexane−methylene chloride solvent mixture to yield 0.5 mg of $Ir_2(CO)_6(\mu\text{-GePh}_2)(GePh_3)_2$[19] (**2**; yield 2%), 2.97 mg of $Ir_3(CO)_6(\eta^1\text{-Ph})_2(\mu\text{-GePh}_2)_3(GePh_3)$ (**3**; yield 16%), 2.5 mg of $Ir_3(CO)_6(\eta^1\text{-Ph})(\mu\text{-GePh}_2)_3(GePh_3)_2$ (**4**; yield 12%), 1.4 mg of $Ir_3(CO)_6(\mu\text{-CO})(\mu\text{-GePh}_2)_2(GePh_3)_3$ (**5**; yield 7%), and 0.4 mg of $Ir_3(CO)_6(\eta^1\text{-Ph})(\mu\text{-GePh}_2)_2(GePh_3)_2[\mu\text{-Ge(Ph)(OH)}]$ (**6**; yield 2%). Spectral data for **3** are as follows. IR ν_{CO} (cm^{-1} in CH_2Cl_2): 1987 (w), 2027 (s), 2048 (w), 2060 (w), 2090 (vw). ^{1}H NMR (in $CDCl_3$): δ 6.67−7.61 (m, 55H, Ph). Mass spectrum: EI-MS showed peaks at m/z 1778 (M − C_6H_6 − CO), 1750 (M − C_6H_6 − 2CO), 1700 (M − $2C_6H_6$ − CO), 1550 (M − $GePh_3$ − CO). Spectral data for **4** are as follows. IR ν_{CO} (cm^{-1} in CH_2Cl_2): 1989 (m), 2021 (s), 2047 (m), 2094 (vw). ^{1}H NMR (in $CDCl_3$): δ 6.67−7.33 (m, 65H, Ph). Mass spectrum: ES^+-MS showed a peak at m/z 2149 (M + K^+). Spectral data for **5** are as follows. IR ν_{CO} (cm^{-1} in CH_2Cl_2): 1869 (m), 1987 (w), 2023 (vs), 2048 (m), 2060 (m), 2097 (w). ^{1}H NMR (in $CDCl_3$): δ 6.64−7.41 (m, 65H, Ph). Mass spectrum: ES^+-MS showed a peak at m/z 2177 (M + K^+). Spectral data for **6** are as follows. IR ν_{CO} (cm^{-1} in CH_2Cl_2): 1996 (w), 2026 (vs), 2050 (m), 2056 (m), 2097 (w). ^{1}H NMR (in $CDCl_3$): δ 6.66−7.33 (m, 65H, Ph), 4.20 (s, 1H, OH). Mass spectrum: EI-MS showed parent ion at m/z 2050. Due to the small amounts of the products, we were unable to obtain elemental analyses.

Conversion of 5 to 4. A 3.2 mg portion (0.002 mmol) of **5** was dissolved in 10 mL of toluene in a 50 mL three-neck flask. The solution was refluxed for 2 h at 110 °C. The solvent was then removed in vacuo, and the products were separated by TLC by using a 4:1 hexane−methylene chloride solvent mixture to yield 2.1 mg of $Ir_3(CO)_6(Ph)(\mu\text{-GePh}_2)_3(GePh_3)_2$ (**4**; yield 68%).

Reaction of 1 with 2 at 110 °C. A 5.5 mg portion (0.006 mmol) of **1** was dissolved in 15 mL of toluene to form a colorless solution in a 50 mL three-neck flask. Then a 7.9 mg (0.005 mmol) amount of **2** was added to this solution. The solution was refluxed for 2.5 h at 110 °C and turned orange. The solvent was then removed in vacuo, and the products were separated by TLC by using a 4:1 hexane−methylene chloride solvent mixture to yield, in order of elution, 4.59 mg of unreacted **2** (58%), 0.90 mg of **3** (13% yield), and trace amounts of some colorless products which could not be characterized.

Thermolysis of 2 at 110 °C. An 8.1 mg portion (0.005 mmol) of **2** was dissolved in 15 mL of toluene in a 100 mL three-neck flask to form a pale yellow solution. The solution was then refluxed for 1.5 h at 110 °C and turned brown. The solvent was removed in vacuo, and the products were separated by TLC by using a 2:1 hexane−methylene chloride solvent mixture to yield 4.2 mg of unreacted $Ir_2(CO)_6(\mu\text{-GePh}_2)(GePh_3)_2$ (53%) and 0.6 mg of **3** (6% yield).

Crystallographic Analyses. Orange crystals of **3** and **4** suitable for single-crystal X-ray diffraction analyses were obtained by slow evaporation of solvent from a methylene chloride−hexane solvent mixture at room temperature. Orange crystals of **5** suitable for X-ray diffraction analyses were obtained by slow evaporation of solvent from a mixture of benzene, octane, and hexane at room temperature. Orange crystals of **6** suitable for X-ray diffraction analyses were obtained by slow evaporation of solvent from a solution of benzene at room temperature. Each data crystal was glued onto the end of a thin glass fiber. X-ray intensity measurements were performed by using a Bruker SMART APEX CCD-based diffractometer using Mo Kα radiation (λ = 0.710 73 Å). The raw data frames were integrated with the SAINT+ program by using a narrow-frame integration algorithm.[20] Corrections for Lorentz and polarization effects were also applied with SAINT+. An empirical absorption correction based on the multiple measurement of equivalent reflections was applied by using the program SADABS. All structures were solved by a combination of direct methods and difference Fourier syntheses , and refined by full-matrix least squares on F^2 by using the SHELXTL software package.[21] All non-hydrogen atoms were refined with anisotropic displacement parameters. All hydrogen atoms on the ligands were placed in geometrically idealized positions and included as standard riding atoms during the least-squares refinements. Crystal data, data collection parameters, and results of the analyses are given in Table 1. Compounds **3** and **5** both crystallized in the triclinic crystal system. The space group $P\bar{1}$ was assumed and confirmed by the successful solution and refinement of the structure. The crystal of **3** contains one independent formula equivalent of the complex and one formula equivalent of hexane that had cocrystallized from the crystallization solvent. The crystal of **5** contains one independent formula equivalent of the complex, one formula equivalent of octane, and a half formula equivalent of hexane cocrystallized from the crystallization solvent. Compound **4** crystallized in the monoclinic crystal system. The space group $P2_1/n$ was confirmed by the pattern of systematic absences observed in the data and the successful solution and refinement of the structure. The crystal of **4** contains one independent formula equivalent of the complex and one formula equivalent of hexane which cocrystallized from the crystallization solvent. Compound **6** also crystallized in the monoclinic crystal system. The space groups $C2/c$ and Cc were indicated by the systematic absences in the data. The centrosymmetric space group $C2/c$ was assumed and confirmed by the successful solution and refinement of the structure. The crystal of **6** contained one independent formula equivalent of the complex and a half formula equivalent of benzene that had cocrystallized from the crystallization solvent. There was disorder in two of the phenyl rings in the structure of **6**.

Computational Details. The DFT calculations were performed by using the TPSS functional[22] as implemented in the Gaussian 09

Table 1. Crystallographic Data for Compounds 3−6

	3	4	5	6
empirical formula	$Ir_3Ge_4C_{72}H_{55}O_6 \cdot C_6H_{14}$	$Ir_3Ge_5C_{84}H_{65}O_6 \cdot C_6H_{14}$	$Ir_3Ge_5C_{85}H_{65}O_7 \cdot 0.5C_6H_{14} \cdot 1.0C_8H_{18}$	$Ir_3Ge_5C_{78}H_{61}O_7 \cdot 0.5C_6H_6$
formula wt	1955.18	2181.97	2270.03	2088.87
cryst syst	triclinic	monoclinic	triclinic	monoclinic
lattice params				
a (Å)	13.9649(4)	16.2440(5)	10.3576(11)	24.9277(10)
b (Å)	15.3595(4)	20.8662(7)	14.9377(16)	20.8199(8)
c (Å)	18.6179(5)	24.0340(8)	29.463(3)	29.1842(11)
α (deg)	68.968(1)	90	86.979(2)	90
β (deg)	77.588(1)	91.129(1)	85.865(2)	94.232(1)
γ (deg)	76.870(1)	90	80.614(2)	90
V (Å^3)	3590.63(17)	8144.8(5)	4481.8(8)	15105.1(10)
space group	$P\bar{1}$	$P2_1/n$	$P\bar{1}$	$C2/c$
Z	2	4	2	8
ρ_{calcd} (g/cm^3)	1.808	1.779	1.682	1.837
μ(Mo Kα) (mm^{-1})	7.238	6.751	6.139	7.277
temp (K)	294(2)	294(2)	294(2)	294(2)
$2\theta_{max}$ (deg)	50.06	48.82	50.06	50.06
no. of obsd rflns ($I > 2\sigma(I)$)	12 693	13 383	15 189	13 350
no. of params	790	790	877	741
goodness of fit (GOF)[a]	1.082	1.086	0.963	1.027
max shift in cycle	0.002	0.001	0.001	0.001
residuals:[a] R1, wR2	0.0476, 0.0980	0.0785, 0.1797	0.0620, 0.2019	0.0422, 0.0988
abs cor, max/min	multiscan, 1.000/0.734	multiscan, 1.000/0.740	multiscan, 1.000/0.672	multiscan, 1.000/0.660
largest peak in final diff map (e/Å^3)	0.953	0.921	3.191	2.156

[a] $R1 = \Sigma_{hkl}(||F_o| - |F_c||)/\Sigma_{hkl}|F_o|$; $wR2 = [\Sigma_{hkl}w(|F_o| - |F_c|)^2/\Sigma_{hkl}wF_o^2]^{1/2}$, $w = 1/\sigma^2(F_o)$; $GOF = [\Sigma_{hkl}w(|F_o| - |F_c|)^2/(n_{data} - n_{vari})]^{1/2}$.

software package.[23] A "double-ζ" quality, effective core potential basis set of Hay and Wadt (LANL2DZ)[24] was employed for the Ir and Ge atoms, and a 6-31G(d) basis set[25] was used for the rest of the atoms. Polarization functions, f and d, were added to Ir and Ge, respectively, and the Ir 6s and 6p functions were modified as suggested by Couty-Hall.[26] The starting geometries for the products were extracted from X-ray crystallographic diffraction analyses. Harmonic vibrational frequency calculations were carried out at the same level of theory after each geometry optimization to confirm all the stable species (zero imaginary frequency) and transition state structures (only one imaginary frequency). All the energy values are reported on the basis of the gas-phase-optimized models.

RESULTS

Five compounds were obtained when a solution of **1** in toluene solvent was heated to reflux at 110 °C for 2.5 h. These include the previously reported diiridium complex $Ir_2(CO)_6(\mu\text{-}GePh_2)(GePh_3)_2$[19] (**2**; 2% yield) and four new triiridium cluster complexes: $Ir_3(CO)_6(\eta^1\text{-}Ph)_2(\mu\text{-}GePh_2)_3(GePh_3)$ (**3**; 16% yield), $Ir_3(CO)_6(\eta^1\text{-}Ph)(\mu\text{-}GePh_2)_3(GePh_3)_2$ (**4**; 12% yield), $Ir_3(CO)_6(\mu\text{-}CO)(\mu\text{-}GePh_2)_2(GePh_3)_3$ (**5**; 7% yield), and $Ir_3(CO)_6(\eta^1\text{-}Ph)(\mu\text{-}GePh_2)_2(GePh_3)_2[\mu\text{-}Ge(Ph)(OH)]$ (**6**; 2% yield). All four of these triiridium compounds were isolated by TLC and characterized by a combination of IR, ^{1}H NMR, mass spectral and single-crystal X-ray diffraction analyses. Compound **2** is the main product obtained by heating $HIr(CO)_3(GePh_3)_2$ at a slightly lower temperature, 104 °C.[19] When the reaction time is extended and the temperature raised to 110 °C, compound **2** is no longer obtained. It seems likely that **2** is at least one intermediate to the triiridium clusters. Indeed, when **2** was heated by itself to 110 °C, it was converted to **3** in 6% yield. Compound **3** was obtained in a better yield (13%) when **2** was combined with **1** and heated to 110 °C.

An ORTEP diagram of the molecular structure of **3** is shown in Figure 1. Compound **3** consists of a triangle of three iridium atoms with one terminal $GePh_3$ ligand, two terminally coordinated σ-phenyl ligands, and three bridging $GePh_2$ ligands, one on each of the three edges of the Ir_3 triangle. The Ir−Ir bond distances in **3** are Ir(1)−Ir(3) = 2.9051(5) Å, Ir(1)−Ir(2) = 2.9430(5) Å, and Ir(2)−Ir(3) = 2.8080(6) Å. The first two distances are similar in length to those of $Ir_3(CO)_6(\mu\text{-}GePh_2)_3(GePh_3)_3$ **7**,[18] 2.9344(4), 2.8971(4), and 2.1935(4) Å, but the last one, Ir(2)−Ir(3), is significantly shorter. The Ir(2)−Ir(3) bond lies between the two σ-phenyl-substituted iridium atoms. The shortness of the Ir(2)−Ir(3) bond may be attributed to decreased steric interactions between the ligands on these two iridium atoms that are less crowded than Ir(1), which contains the bulky $GePh_3$ ligand. The Ir−Ge distance to the $GePh_3$ ligand on Ir(1), Ir(1)−Ge(4) = 2.5490(11) Å, is similar to the Ir−Ge distances to the $GePh_3$ ligands in the related triiridium compound (**7**): 2.5754(7), 2.5959(7), and 2.5534(8) Å.[18] The Ir−Ge bond distances to the bridging $GePh_2$ ligands in **3** are slightly different. The Ir−Ge bond distances to the bridging $GePh_2$ ligands bonded to Ir(1), Ir(1)−Ge(1) = 2.5386(11) Å and Ir(1)−Ge(3) = 2.5598(11) Å, are significantly longer than those to Ir(2) and Ir(3): Ir(2)−Ge(1) = 2.4871(12) Å, Ir(2)−Ge(2) = 2.5055(12) Å, Ir(3)−Ge(2) = 2.5003(11) Å, and Ir(3)−Ge(3) = 2.4765(11) Å. The longer Ir−Ge distances to Ir(1) could also be due to the steric effects produced by the bulky $GePh_3$ ligand on that atom.

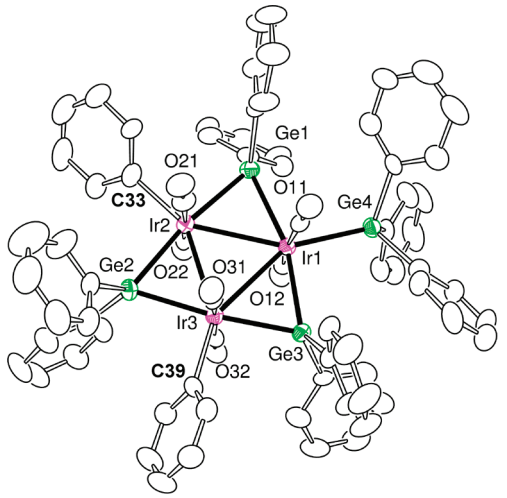

Figure 1. ORTEP diagram of the molecular structure of compound **3**, showing 30% probability thermal ellipsoids. Selected bond distances (in Å) are as follows: Ir(1)−Ir(3) = 2.9051(5), Ir(1)−Ir(2) = 2.9429(5), Ir(2)−Ir(3) = 2.8080(6), Ir(1)−Ge(1) = 2.5386(11), Ir(1)−Ge(3) = 2.5598(11), Ir(1)−Ge(4) = 2.5490(11), Ir(2)−Ge(1) = 2.4871(12), Ir(2)−Ge(2) = 2.5055(12), Ir(3)−Ge(2) = 2.5003(11), Ir(3)−Ge(3) = 2.4765(11), Ir(2)−C(33) = 2.127(11), Ir(3)−C(39) = 2.130(10).

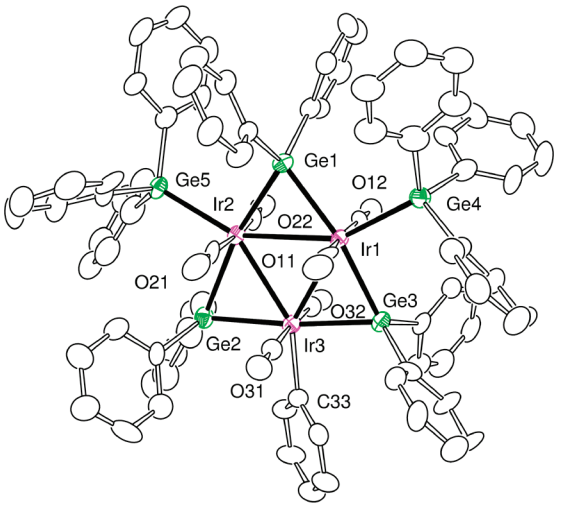

Figure 2. ORTEP diagram of the molecular structure of compound **4**, showing 30% probability thermal ellipsoids. Selected bond distances (in Å) are as follows: Ir(1)−Ir(3) = 2.8554(9), Ir(1)−Ir(2) = 2.9503(9), Ir(2)−Ir(3) = 2.8584(9), Ir(1)−Ge(1) = 2.5266(19), Ir(1)−Ge(3) = 2.5385(19), Ir(1)−Ge(4) = 2.551(2), Ir(2)−Ge(1) = 2.520(2), Ir(2)−Ge(2) = 2.535(2), Ir(2)−Ge(5) = 2.5519(19), Ir(3)−Ge(2) = 2.490(2), Ir(3)−Ge(3) = 2.4915(19), Ir(3)−C(33) = 2.127(18).

The Ir(1)−C distances to the σ-phenyl ligands are Ir(2)−C(33) = 2.127(11) Å and Ir(3)−C(39) = 2.130(10) Å. These distances are similar to the Ir−C distances to the phenyl ligands in the Ir_3, Ir_4, and Ir_8 complexes $Ir_3(CO)_9(Ph)(\mu_3\text{-PPh})(\mu\text{-dppm})$ (2.084(16) Å),[27] $Ir_4(CO)_8(\eta^1\text{-Ph})[\mu_4\text{-}\eta^3\text{-PhPC(H)CPh}](\mu\text{-PPh}_2)$ (2.09(1) Å),[28] and $Ir_8(CO)_{16}(\eta^1\text{-Ph})(\mu\text{-PPh}_2)(\mu_4\text{-PPh})$ (2.06(4) Å).[29]

An ORTEP diagram of the molecular structure of **4** is shown in Figure 2. Compound **4** is similar to compound **3**, but instead of one terminal $GePh_3$ and two terminal σ-phenyl ligands, it contains two terminal $GePh_3$ ligands and one terminal σ-phenyl ligand. The Ir−Ir bond distances are similar to those in **2**, Ir(1)−Ir(3) = 2.8554(9) Å, Ir(1)−Ir(2) = 2.9503(9) Å, and Ir(2)−Ir(3) = 2.8584(9) Å, but the Ir(1)−Ir(2) distance is notably longer than the other two distances. As in **3**, this may be attributed to steric effects, because Ir(1) and Ir(2) both contain a bulky terminal $GePh_3$ ligand while Ir(3) contains the less bulky σ-phenyl ligand. There are similar effects on the bond distances to the bridging $GePh_2$ ligands. The Ir−C distance to the σ-phenyl ligand, Ir(3)−C(33) = 2.127(18) Å, is quite similar to the Ir−phenyl distances in compound **3**, 2.127(11) and 2.130(10) Å.

An ORTEP diagram of the molecular structure of **5** is shown in Figure 3. Compound **5** is the only triiridium compound that has only two bridging $GePh_2$ ligands. In this compound there is a bridging CO ligand on the third Ir−Ir bond. The three Ir−Ir bond distances are similar to those in **3**, with the exception that the CO-bridged Ir−Ir bond, Ir(1)−Ir(2) = 2.7826(7) Å, is significantly shorter than the other two, Ir(1)−Ir(3) = 2.8927(7) Å and Ir(2)−Ir(3) = 2.9281(7) Å. There are three terminal $GePh_3$ ligands, one on each iridium atom. The Ir−Ge bond distances to the $GePh_3$ ligands are similar to those in **3** and **4**: Ir(1)−Ge(1) = 2.5098(14) Å, Ir(2)−Ge(2) = 2.5155(16) Å, and Ir(3)−Ge(3) = 2.5401(15) Å. The Ir−Ge bond distances to the bridging $GePh_2$ ligands are also similar to those in **3** and **4**: Ir(3)−Ge(4) = 2.5428(14) Å, Ir(3)−Ge(5) = 2.5318(15) Å,

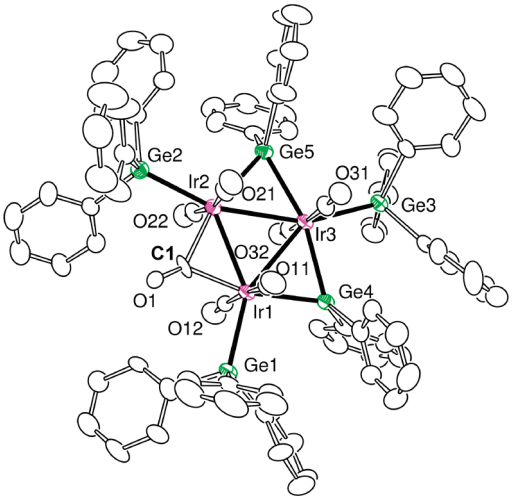

Figure 3. ORTEP diagram of the molecular structure of compound **5**, showing 30% probability thermal ellipsoids. Selected bond distances (in Å) are as follows: Ir(1)−Ir(2) = 2.7826(7), Ir(1)−Ir(3) = 2.8927(7), Ir(2)−Ir(3) = 2.9281(7), Ir(1)−Ge(1) = 2.5098(14), Ir(1)−Ge(4) = 2.5131(15), Ir(2)−Ge(5) = 2.5059(15), Ir(2)−Ge(2) = 2.5155(16), Ir(3)−Ge(5) = 2.5318(15), Ir(3)−Ge(3) = 2.5401(15), Ir(3)−Ge(4) = 2.5428(14), Ir(1)−C(1) = 2.124(14), Ir(2)−C(1) = 2.131(13).

Ir(1)−Ge(4) = 2.5131(15) Å, and Ir(2)−Ge(5) = 2.5059(15) Å. Interestingly, we were able to obtain compound **4** from **5** in 68% yield by heating a solution of **5** in toluene to reflux for 2 h.

An ORTEP diagram of the molecular structure of **6** is shown in Figure 4. Compound **6** is most similar to compound **4** in having three bridging germylene ligands, two terminal $GePh_3$ ligands, and one terminal σ-phenyl ligand. Unlike **4**, one of the bridging germylene ligands contains an OH group instead of a second phenyl group: i.e., it is Ge(OH)(Ph) instead of $GePh_2$, Ge(1)−O(1) = 1.797(6) Å. The resonance of the hydrogen

atom H(1) on the oxygen atom O(1) was observed in the ^{1}H NMR spectrum at δ 4.20 (s, 1H, OH). The Ir−Ir bond distances are similar to those in **4**, Ir(1)−Ir(2) = 2.8572(5) Å, Ir(1)−Ir(3) = 2.9475(5) Å, and Ir(2)−Ir(3) = 2.8560(5) Å, but the Ge(OH)(Ph)-bridged Ir−Ir bond distance is significantly longer than the other two. We believe that compound **6** is a hydrolysis product of one of the preceding Ir_3Ge_5 products **4** or **5**, but we have not been able to confirm that in this study.

DISCUSSION

A summary of the results obtained in this study is shown in Scheme 3. The thermolysis of **1** leads to ligand loss and the formation of the di- and triiridium complexes **2**−**6**. All of the complexes contain bridging germylene ligands formed by the cleavage of a phenyl group from the triphenylgermyl ligands in **1**. In previous studies, we have shown that bridging germylene ligands are readily formed by cleavage of phenyl groups from $GePh_3$ ligands in metal carbonyl complexes. When hydride ligands are present in the complexes, the cleavage of the phenyl group is accompanied by the formation of benzene by combination with a hydride ligand.[5]

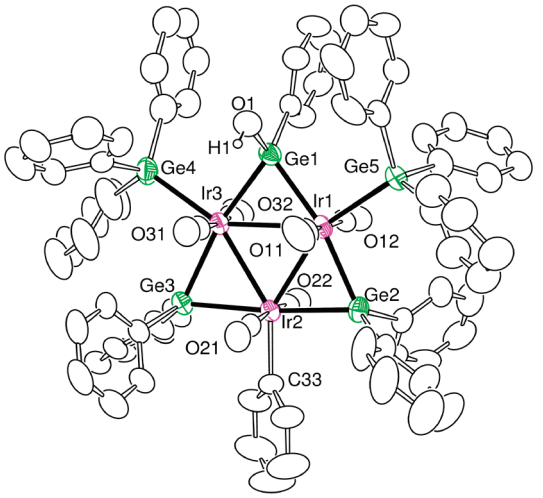

Figure 4. ORTEP diagram of the molecular structure of compound **6**, showing 30% probability thermal ellipsoids. Selected bond distances (in Å) are as follows: Ir(1)−Ir(2) = 2.8572(5), Ir(1)−Ir(3) = 2.9475(5), Ir(2)−Ir(3) = 2.8560(5), Ir(1)−Ge(1) = 2.5044(11), Ir(1)−Ge(2) = 2.5325(11), Ir(1)−Ge(5) = 2.5391(9), Ir(2)−Ge(2) = 2.4862(10), Ir(2)−Ge(3) = 2.5091(10), Ir(3)−Ge(1) = 2.4793(9), Ir(3)−Ge(3) = 2.5319(9), Ir(3)−Ge(4) = 2.5428(12), Ir(2)−C(33) = 2.118(9), Ge(1)−O(1) = 1.797(6).

It is anticipated that the formation of the bridging $GePh_2$ ligands in compounds **2**−**6** are formed by similar α-cleavage processes, but the mechanism(s) of the cleavage of phenyl groups from $GePh_3$ ligands has not been established or discussed in any previous studies; Tilley has described the mechanism of the α-cleavage of phenyl groups from $SnPh_3$ ligands in mononuclear bis-cyclopentadienyl hafnium complexes (eq 2).[7] Compounds **3**, **4**, and **6** each have at least one σ-phenyl ligand coordinated to one of the iridium atoms in the cluster. Interestingly, we have found that compound **5** was converted into **4** in good yield by a thermal decarbonylation at 110 °C. In the process the bridging CO ligand was replaced by a bridging $GePh_2$ ligand. The $GePh_2$ ligand was evidently generated by an α-cleavage of a phenyl ring from one of the $GePh_3$ ligands on one of the iridium atoms that was bonded to the bridging CO ligand. The phenyl ring remains as a σ-bonded ligand where the $GePh_3$ ligand was originally coordinated.

In 1984 Hoffmann investigated the nature of alkyl and aryl shifts from tertiary phosphine ligands to 16-electron d^8 transition metals.[30] It was concluded that the transformation was "allowed" and occurred by a migration mechanism. All of the iridium atoms in **5** have 18-electron configurations, and so the decarbonylation and phenyl-cleavage to transform **5** into **4** has provided a unique opportunity to study the mechanism of the α-cleavage process in a polynuclear metal environment with electronically saturated metal atoms. To investigate the mechanism of this α-phenyl cleavage transformation of **5** into **4**, we have performed a series of geometry-optimized DFT computations. Selected molecular orbitals for **5** are shown in Figure 5. Complex **5** can be viewed as a combination of three Ir(III) atoms, each with five main-group ligands: $[GePh_3]^-$, $[GePh_2]^{2-}$, and $[CO]^{2-}$. Thus, these three Ir fragments can be thought of as t_{2g}^6 O_h fragments with one ligand missing. The symmetric A_1 HOMO forms one of the three Ir−Ir bonding MOs and is the completely in-phase combination of three in-plane "d^2sp^3" (O_h hybrids), one from each iridium atom that is directed toward the center of the cluster. This orbital has much more Ir 6p than 5d character, with substantial contributions from the π^* of the terminal CO

Scheme 3

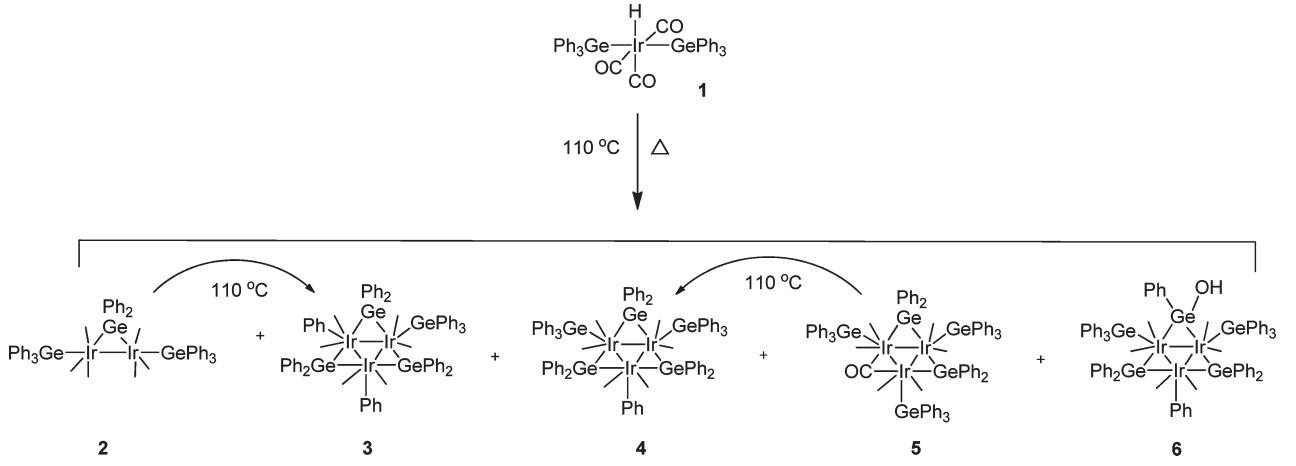

ligands. The other two Ir—Ir bonding MOs are lower in energy and are composed of two combinations of in-plane d_{xy} orbitals from each Ir atom. This d_{xy} orbital is the least stable of the three t_{2g}-like orbitals that were occupied on each Ir atom. When the cluster forms, the totally antibonding combination of these three Ir d_{xy} orbitals is destabilized such that it rises above the HOMO and becomes the empty LUMO of the cluster. The HOMO-1 at −5.37 eV consists of Ir—Ge interactions to the bridging $GePh_2$ ligands and the Ir—C interactions to the bridging CO ligand.

Our analysis has revealed that the transformation of **5** to **4** is initiated by the loss of a CO ligand which generates the electronic unsaturation about the metal atoms that subsequently facilitates the cleavage of a Ge—C bond to one of the phenyl groups at one of the metal atoms. There are two types of CO ligands in the proximity of the site that the newly formed bridging $GePh_2$ ligand will occupy: these are the bridging CO ligand and the

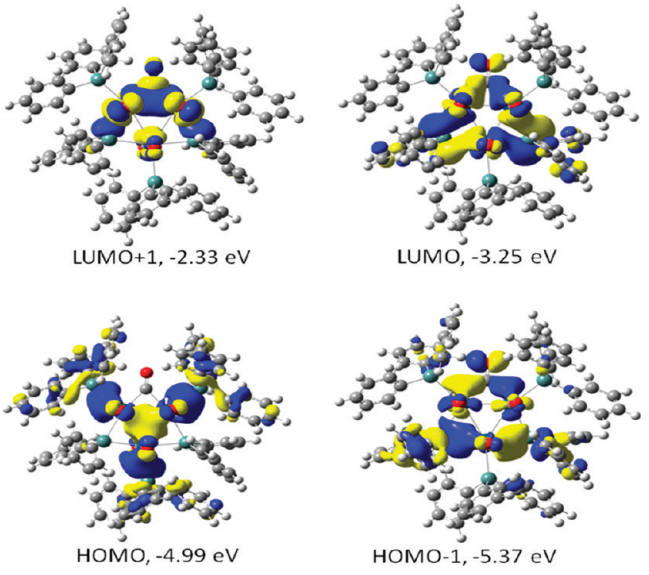

Figure 5. Frontier molecular orbitals for compound **5**.

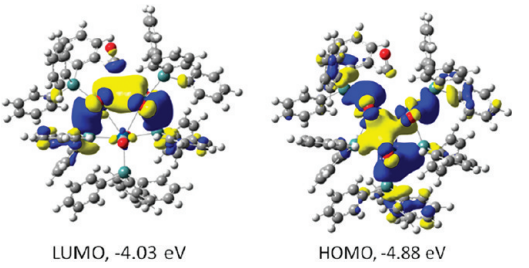

Figure 7. HOMO and LUMO for transition state $TS_{5,A}$.

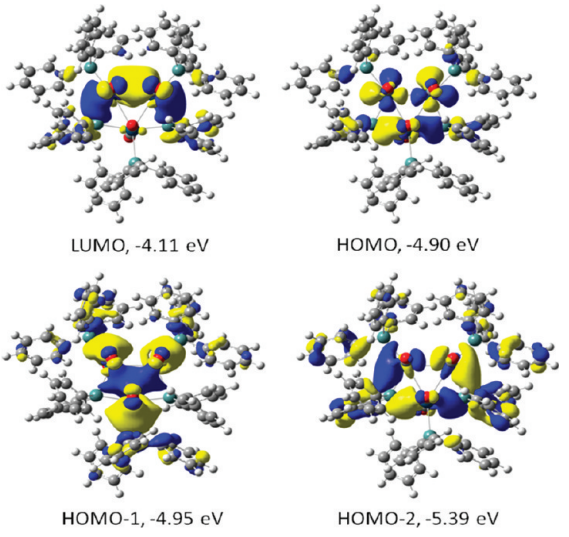

Figure 8. Selected molecular orbitals for the intermediate A.

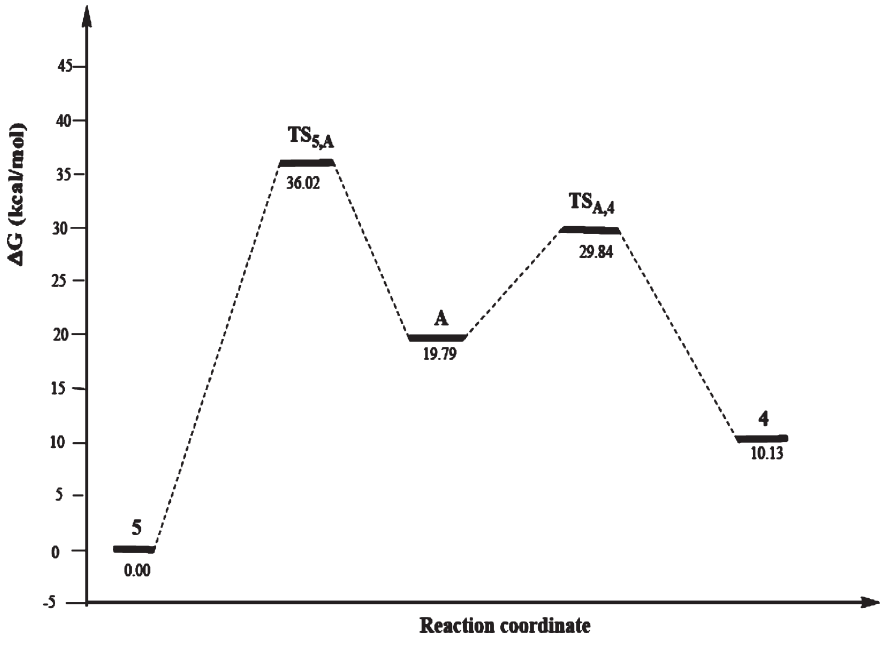

Figure 6. Energy level diagram of the species formed in the course of the transformation of compound **5** to **4**.

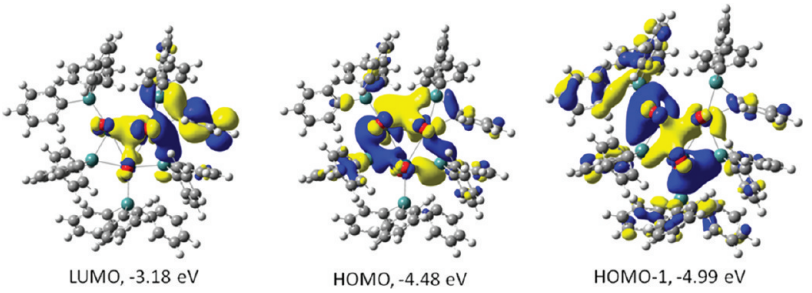

Figure 9. LUMO, HOMO, and HOMO-1 for transition state $TS_{A,4}$.

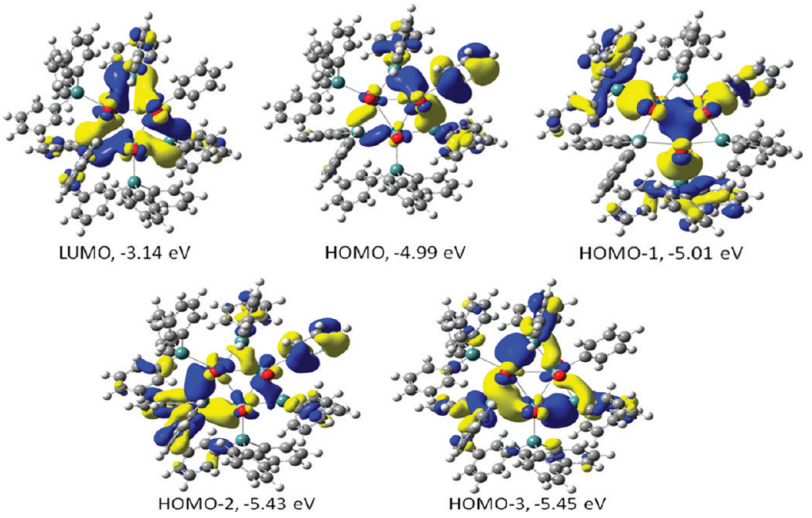

Figure 10. Frontier molecular orbitals for **4**.

terminal CO ligands on the two iridium atoms that are bonded to the bridging CO ligand.

Our analysis has indicated that dissociation of the bridging CO ligand is approximately 3.0 kcal/mol lower in energy than the dissociation of one of four proximate terminal CO ligands. We have obtained a structure for a transition state, $TS_{5,A}$, $\Delta G^{\ddagger} = 36.02$ kcal/mol, en route to the intermediate $Ir_3(CO)_6(\mu\text{-}GePh_2)_2(GePh_3)_3$ (**A**), which lies 19.79 kcal/mol higher in energy than **5** (see the reaction profile in the energy level diagram in Figure 6). The frontier orbitals of $TS_{5,A}$ are shown in Figure 7. The bridging CO ligand has moved away from the two iridium atoms to which it was bonded. The Ir—C distances to this departing CO ligand are approximately 3.75 Å in $TS_{5,A}$. The LUMO, HOMO, and HOMO-1 of intermediate **A** are shown in Figure 8. The major component of the LUMO of **A** lies where the bridging CO ligand was located. Upon elimination of the CO ligand, the LUMO+1 of **5** falls in energy as it was being pushed up by the CO lone pair and becomes the in-plane Ir—Ir bonding orbital, now the LUMO of the intermediate. In addition, the Ir—Ir orbital that was being stabilized by the in-plane π^* orbital of the CO and was the HOMO-1 of **5** rises in energy and becomes the HOMO of **A**; this HOMO is Ir—Ir antibonding. If these two orbitals had changed in energy enough to switch places, there would be an Ir—Ir double bond here.

The most interesting step in the transformation of **5** to **4** is the cleavage of the Ge—C bond to one of the phenyl ligands in the selected $GePh_3$ ligand on one of the iridium atoms that was bonded to the bridging CO ligand in **5**. This transformation proceeds through the transition state $TS_{A,4}$. In the course of this rearrangement, the germanium atom is shifted toward the site where the bridging CO ligand was located in **5** and one of the phenyl groups on the Ge atom forms an agostic bonding interaction to the iridium atom, resulting in an η^2-$GePh_3$ ligand with Ir—Ge = 2.56 Å, Ir—C = 2.45 Å, and Ge—C = 2.09 Å. The LUMO, HOMO, and HOMO-1 of $TS_{A,4}$ are shown in Figure 9.

In the formation of $TS_{A,4}$, the Ir—Ge bond in A attacks the LUMO and becomes the HOMO of $TS_{A,4}$, where the formation of the new Ir—Ge bond is obvious. The new Ir—Ph bond forms from the flow of electrons from the HOMO of the intermediate into the Ge—Ph antibonding orbital. However, the formation of this new Ir—Ph bond is not easily seen in these MO's, because $TS_{A,4}$ is a very early transition state, i.e. the Ge—Ph bond has lengthened by only 0.1 Å, while the Ir—Ph distance is still 0.3 Å longer than its final length in **4**. The frontier molecular orbitals for **4** are shown in Figure 10. The bond to the σ-phenyl ligand is fully established and is readily apparent in the HOMO-1. The bonding to the three bridging $GePh_2$ ligands is shown clearly in the HOMO, HOMO-2, and the HOMO-3.

Overall, this mechanism is similar to the "deinsertion" decarbonylation process, i.e. a reverse of the "insertion" mechanism, one of two mechanisms that was described by Noack and Calderazzo many years ago in their studies of the formation of the acetyl ligand by the combination of methyl groups with CO

Scheme 4

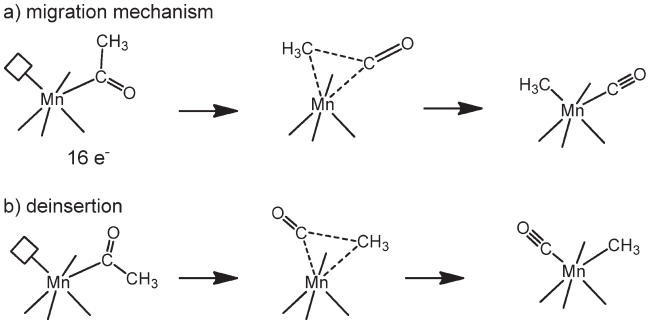

ligands in methylmanganese carbonyl complexes.[31] Their studies of the formation of the acetyl ligands in these complexes indicated that the mechanism that was most consistent with experimental data was the "migratory" process in which the methyl group moved from its original coordination site to the carbon of the CO ligand, as opposed to the alternative "insertion" mechanism in which the CO ligand was shifted from its coordination site into the M−C bond to the methyl group at the site of coordination of the methyl group. The microscopic reverse of the migration process is shown in Scheme 4a, in which the methyl group changes sites, and the "deinsertion" (reverse of the insertion mechanism) in Scheme 4b, in which the CO group changes sites.

The α-cleavage of the phenyl group from the $GePh_3$ ligand in **5** leaves the phenyl group at the site where the $GePh_3$ was originally coordinated and the $GePh_2$ group has moved to the site where the bridging CO ligand was located, see Scheme 5. This transformation is most comparable to the "deinsertion" mechanism shown in Scheme 4b.

Scheme 5

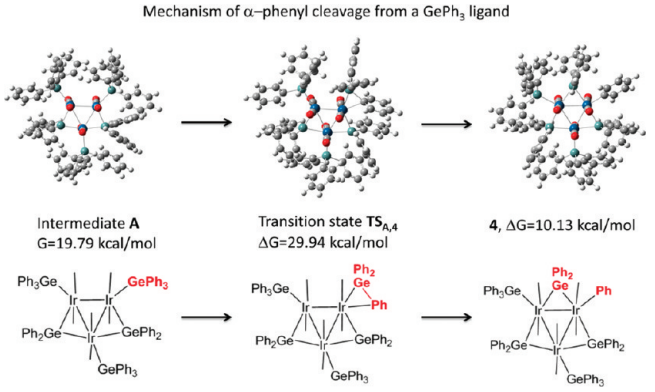

SUMMARY

In this work we have prepared a series of new triiridium cluster complexes containing bridging $GePh_2$ ligands in low yields by a combination of condensation reactions and phenyl cleavage processes from the $GePh_3$ ligands in the starting complex **1**. Interestingly, the reaction of **1** with $HGePh_3$ at only slightly lower temperatures, i.e. 104 °C, yielded principally the known diiridium complexes $H_2Ir_2(CO)_4(\mu\text{-}GePh_2)_2(GePh_3)$ and $Ir_2(CO)_8[\mu\text{-}Ph_2Ge(OH)GePh_2](\mu\text{-}GePh_2)(GePh_3)_2(\mu\text{-}H)$.[19] Compound **3** was also obtained by heating compound **2** or by heating a mixture of **1** and **2** at 110 °C. Compound **5** was converted to **4** by loss of CO and a α-cleavage of a phenyl group from one of its $GePh_3$ ligands when it was heated to 110 °C in a toluene solution. A viable intramolecular deinsertion mechanism for the phenyl α-cleavage process was established by a series of sophisticated DFT computational analyses. This mechanism may have implications in similar cleavage processes for a range of other ligands containing phenyl groups.[2,7] If their yields can be improved, these new germanium−triiridium complexes may be able to serve as precursors to new IrGe heterogeneous nanocatalysts for hydrogenation reactions or hydrocarbon-based reforming processes.[11,12,15,16]

ASSOCIATED CONTENT

Supporting Information. Text giving computational details and CIF files giving crystallographic data for each of the structural analyses. This material is available free of charge via the Internet at http://pubs.acs.org.

AUTHOR INFORMATION

Corresponding Authors

*E-mail: Adams@chem.sc.edu; Hall@science.tamu.edu.

ACKNOWLEDGMENT

This research was supported by the National Science Foundation (Grant No. CHE-1111496, R.D.A.) and the USC Nanocenter. The authors from Texas A&M University gratefully acknowledge the National Science Foundation (Grant Nos. CHE-0541587 and CHE-0910552) and the Welch Foundation (Grant A-0648) for support.

REFERENCES

(1) (a) Bruce, M. I.; Zaitseva, N. N.; Skelton, B. W.; White, A. H. *J. Organomet. Chem.* **1996**, *515*, 143. (b) Bradford, C. W.; Nyholm, R. S.; Gainsford, G. J.; Guss, J. M.; Ireland, P. R.; Mason, R. *J. Chem. Soc., Chem. Commun.* **1972**, 87. (c) Gainsford, G. J.; Guss, J. M.; Ireland, P. R.; Mason, R.; Bradford, C. W.; Nyholm, R. S. *J. Organomet. Chem.* **1972**, *40*, C70. (d) Deeming, A. J.; Kabir, S. E.; Underhill, M. *J. Chem. Soc., Dalton Trans.* **1973**, 2589. (e) Deeming, A. J.; Rothwell, I. P.; Hursthouse, M. B.; Backer-Dirks, J. D. *J. Chem. Soc., Dalton Trans.* **1981**, 1879. (f) Brown, S. C.; Evans, J.; Webster, M. J. *J. Chem. Soc., Dalton Trans.* **1980**, 1021. (g) Adams, R. D.; Captain, B.; Fu, W.; Smith, M. D. *J. Organomet. Chem.* **2002**, *651*, 124–131.

(2) Garrou, P. E. *Chem. Rev.* **1985**, *85*, 171–185.

(3) (a) Adams, R. D.; Captain, B.; Pearl, W. C., Jr. *J. Organomet. Chem.* **2008**, *693*, 1636–1644. (b) Leong, W. K.; Chen, G. *Organometallics* **2001**, *20*, 2280–2287. (c) Leong, W. K.; Chen, G. *J. Cluster Sci.* **2006**, *17*, 111.

(4) (a) Adams, R. D.; Pearl, W. C., Jr. *Inorg. Chem.* **2010**, *49*, 7170–7175. (b) Adams, R. D.; Pearl, W. C., Jr. *Inorg. Chem.* **2009**, *48*, 9519–9525.

(5) Adams, R. D.; Captain, B.; Zhu, L. *Inorg. Chem.* **2005**, *44*, 6623–6631.

(6) Adams, R. D.; Kan, Y.; Zhang, Q. *Organometallics* **2011**, *30*, 328–333.

(7) Neale, N. R.; Tilley, T. D. *J. Am. Chem. Soc.* **2005**, *127*, 14745–14755.

(8) (a) Adams, R. D.; Trufan, E. *Philos. Trans. R. Soc.* **2010**, *368*, 1473–1493. (b) Adams, R. D.; Captain, B.; Herber, R. H.; Johansson, M.; Nowik, I.; Smith, J. L., Jr.; Smith, M. D. *Inorg. Chem.* **2005**, *44*, 6346–6358. (c) Adams, R. D.; Kan, Y.; Trufan, E.; Zhang, Q. *J. Cluster Sci.* **2010**, *21*, 371–378.

(9) (a) Adams, R. D.; Captain, B.; Trufan, E. *J. Organomet. Chem.* **2008**, *693*, 3593–3602. (b) Adams, R. D.; Captain, B.; Trufan, E. *J. Cluster Sci.* **2007**, *18*, 642–659. (c) Adams, R. D.; Captain, B.; Fu, W. *Inorg. Chem.* **2003**, *42*, 1328–1333. (d) Adams, R. D.; Boswell, E. M.; Captain, B.; Patel, M. A. *Inorg. Chem.* **2007**, *46*, 533–540. (e) Adams, R. D.; Trufan, E. *Inorg. Chem.* **2009**, *48*, 6124–6129. (f) Adams, R. D.; Trufan, E. *Inorg. Chem.* **2010**, *49*, 3029–3034.

(10) (a) Hungria, A. B.; Raja, R.; Adams, R. D.; Captain, B.; Thomas, J. M.; Midgley, P. A.; Golvenko, V.; Johnson, B. F. G. *Angew. Chem., Int. Ed.* **2006**, *45*, 4782–4785. (b) Adams, R. D.; Boswell, E. M.; Captain, B.; Hungria, A. B.; Midgley, P. A.; Raja, R.; Thomas, J. M. *Angew. Chem., Int. Ed.* **2007**, *46*, 8182–8185. (c) Adams, R. D.; Blom, D. A.; Captain, B.; Raja, R.; Thomas, J. M.; Trufan, E. *Langmuir* **2008**, *24*, 9223–9226. (d) Yang, F.; Trufan, E.; Adams, R. D.; Goodman, D. W. *J. Phys. Chem. C* **2008**, *112*, 14233–14235.

(11) (a) Sinfelt, J. H. *Sci. Am.* **1985**, *253*, 90–98.(b) Sinfelt, J. H., In *Bimetallic Catalysts. Discoveries, Concepts and Applications*; Wiley: New York, 1983. (c) Sinfelt, J. H.; Via, G. H. *J. Catal.* **1979**, *56*, 1–11. (d) Rasser, J. C.; Beindorff, W. H.; Scholten, J. J. F. *J. Catal.* **1979**, *59*, 211–222.(e) Ponec, V. Bond, G. C. In *Catalysis by Metals and Alloys*; Elsevier: Amsterdam, 1998; Studies in Surface Science and Catalysis 95, Chapter 13.

(12) (a) Gates, B. C. *Chem. Rev.* **1995**, *95*, 511–522. (b) Mondloch, J. E.; Finke, R. G. *J. Am. Chem. Soc.* **2011**, *133*, 7744–7756. (c) Alexeev, O.; Gates, B. C. *Ind. Eng. Chem. Res.* **2003**, *42*, 1571–1587.

(13) Crabtree, R. H. *Top. Organomet. Chem.* **2011**, *34*, 1–10.

(14) Jones, J. H. *Platinum Met. Rev.* **2000**, *44*, 94–105.

(15) Macleod, N.; Fryer, J. R.; Stirling, D.; Webb, G. *Catal. Today* **1998**, *46*, 37–54.

(16) (a) Ekou, T.; Vicente, A.; Lafaye, G.; Especel, C.; Marecot, P. *Appl. Catal. A: Gen.* **2006**, *314*, 73–80. (b) Lafaye, G.; Micheaud-Especel, C.; Montassier, C.; Marecot, P. *Appl. Catal. A: Gen.* **2002**, *230*, 19–30. (c) Lafaye, G.; Micheaud-Especel, C.; Montassier, C.; Marecot, P. *Appl. Catal. A: Gen.* **2004**, *257*, 107–117.

(17) Hawkins, S. M.; Hitchcock, P. B.; Lappert, M. F.; Rai, A. K. *Chem. Commun.* **1986**, 1689–1690.

(18) Adams, R. D.; Captain, B.; Smith, J. L., Jr. *Inorg. Chem.* **2005**, *44*, 1413–1420.

(19) Adams, R. D.; Trufan, E. *Organometallics* **2010**, *29*, 4346–4353.

(20) *SAINT+, version 6.2a*; Bruker Analytical X-ray Systems, Inc., Madison, WI, 2001.

(21) Sheldrick, G. M. *SHELXTL, version 6.1*; Bruker Analytical X-ray Systems, Inc., Madison, WI, 1997.

(22) Tao, J.; Perdew, J. P.; Staroverov, V. N.; Scuseria, G. E. *Phys. Rev. Lett.* **2003**, *91*, 146401–146404.

(23) Calculations were performed by using the Gaussain09 and Amsterdam Density Functional (ADF) program packages. See the Supporting Information.

(24) (a) Hay, P. J.; Wadt, W. R. *J. Chem. Phys.* **1985**, *82*, 284–298. (b) Hay, P. J.; Wadt, W. R. *J. Chem. Phys.* **1985**, *82*, 270–283. (c) Hay, P. J.; Wadt, W. R. *J. Chem. Phys.* **1985**, *82*, 299–310.

(25) (a) Hehre, W. J.; Ditchfield, R.; Pople, J. A. *J. Chem. Phys.* **1972**, *56*, 2257–2261. (b) Hariharan, P. C.; Pople, J. A. *Theor. Chem. Acc.* **1973**, *28*, 213–222.

(26) (a) Couty, M.; Hall, M. B. *J. Comput. Chem.* **1996**, *17*, 1359–1370. (b) Ehlers, A. W.; Biihme, M.; Dapprich, S.; Gobbi, A.; Hijllwarth, A.; Jonas, V.; Kiihler, K. F.; Stegmann, R.; Veldkamp, A.; Frenking, G. *Chem. Phys. Lett.* **1993**, *208*, 111–114. (c) Höllwarth, A.; Biihme, M.; Dapprich, S.; Ehlers, A. W.; Gobbi, A.; Jonas, V.; Köhler, K. F.; Stegmann, R.; Veldkamp, A.; Frenking, G. *Chem. Phys. Lett.* **1993**, *208*, 237–240.

(27) Harding, M. M.; Nicholls, B. S.; Smith, A. K. *J. Chem. Soc., Dalton Trans.* **1983**, 1479–1481.

(28) Pereira, R. M. S.; Fujiwara, F. Y.; Vargas, M. D. *Organometallics* **1997**, *16*, 4833–4838.

(29) de Araujo, M. H.; M., D.; Braga, D.; Grepioni, F. *Polyhedron* **1998**, *17*, 2865–2875.

(30) Ortiz, J. V.; Havlas, Z.; Hoffmann, R. *Helv. Chim. Acta* **1984**, *67*, 1–17.

(31) (a) Noack, K.; Calderazzo, F. *J. Organomet. Chem.* **1967**, *10*, 101–104. (b) Calderazzo, F.; Noack, K. *Coord. Chem. Rev.* **1966**, *1*, 118–125.